Received: 25 June 2021 | Revised: 31 August 2021 | Accepted: 6 September 2021

DOI: 10.1002/ppap.202100097

RESEARCH ARTICLE

PLASMA PROCESSES AND POLYMERS

Inhibition of biofilm formation on polystyrene substrates by atmospheric pressure plasma polymerization of siloxane-based coatings

Rodolfo Múgica-Vidal[1] | **Elisa Sainz-García**[1] | **Ignacio Muro-Fraguas**[1] | **Ana Sainz-García**[1] | **Ana González-Marcos**[1] | **María López**[2] | **Beatriz Rojo-Bezares**[2] | **Paula Toledano**[2] | **Yolanda Sáenz**[2] | **Fernando Alba-Elías**[1]

[1]Department of Mechanical Engineering, University of La Rioja, Logroño, Spain

[2]Molecular Microbiology Area, Center for Biomedical Research of La Rioja (CIBIR), Logroño, Spain

Correspondence
Rodolfo Múgica-Vidal, Department of Mechanical Engineering, University of La Rioja, c/San José de Calasanz 31, Logroño 26004, La Rioja, Spain.
Email: rodolfo.mugica@unirioja.es

Funding information
Ministerio de Ciencia e Innovación, Grant/Award Number: PID2020-113658RB-C21

Abstract

Biofilms pose important economic and health risks in biomedical applications and in food industries. In this study, coatings that reduce the biofilm formation of *Pseudomonas aeruginosa* on polystyrene cell culture plates are deposited by plasma polymerization of (3-aminopropyl)triethoxysilane using an atmospheric pressure plasma jet system at three different power levels. Surface characterizations and quantification of biofilm formation during 1 week after deposition suggest that the higher concentration of oxygenated carbon groups on the coated samples than on uncoated ones can induce higher levels of oxidative stress in the bacteria in contact with the coatings. This causes an initial overproduction of extracellular polymeric substances that can avoid further bacterial attachment and biofilm formation at later cycles of biofilm development.

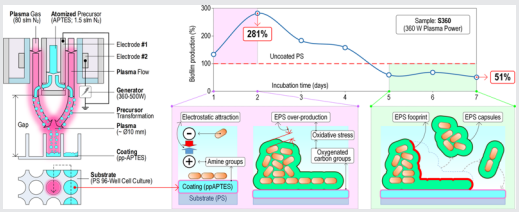

KEYWORDS
aminopropyltriethoxysilane, antibacterial coatings, atmospheric pressure plasma jet, biofilm, plasma polymerization

1 | INTRODUCTION

Biofilms are defined as organized bacterial communities embedded in an extracellular polymeric matrix attached to living or abiotic surfaces. Bacterial biofilms are a matter of concern in industrial and medical applications because this capacity provides advantages to bacteria to colonize and multiply in different environments. Numerous studies have underlined that healthcare-associated infections and foodborne diseases are mainly caused by the biofilms formed on equipment surfaces of both food and medical fields. Food, water systems, and industrial sectors provide suitable environments for biofilm formation, which compromises food safety causing cross-contamination of the final products, impacts the deterioration and the failure of the industrial materials, and increases the public health risk.[1,2] Additionally, these bacterial communities have an enormous clinical impact, being recognized as one of the major determinants in nosocomial and persistent infections. They contaminate medical devices, implants, catheters, and cannulas that interact with the human body during and after surgical intervention.[3,4]

The biofilm formation begins when planktonic bacteria attach to a conditioned surface (Figure 1a). The attached bacteria produce a matrix of extracellular polymeric substances (EPS), such as polysaccharides and proteins, which facilitate surface colonization and bacterial aggregation (Figure 1b). Then, the biofilm matures and develops a three-dimensional structure. Bacteria from a mature biofilm detach and spread to colonize new areas, thus causing biofilm dispersal (Figure 1c).[2,3,5]

Since the EPS matrix provides protection against the external environment, biofilm-growing bacteria show higher resistance to antibiotics and host defenses than planktonic bacteria.[2,6–8] Due to their high persistence, biofilms are also the cause of important economic costs associated with the replacement of infected devices and the removal of implants.[9–11]

Pseudomonas aeruginosa is an opportunistic Gram-negative pathogen, with great metabolic versatility and extraordinary ability to grow in varied and daily environments. *P. aeruginosa* represents a significant health problem in the hospital environment because it causes approximately 75% of the biofilm-related infections linked to medical devices and implants.[11] Additionally, it is one of the most common pathogens in the food industry because of its presence in soil, water, animals, and plants.[2] This ubiquitous bacterium is a model microorganism for the study and control of bacterial biofilms.

Traditional methods to combat biofilms require the use of toxic chemicals or excessively high concentrations of antibiotics, so many efforts are being invested in the development of novel approaches to prevent biofilm formation, mainly focused on avoiding bacterial attachment. In this regard, the use of plasma technologies for surface treatment and coating deposition has become an interesting approach, as they are able to modify the surface characteristics while keeping the bulk properties of the substrate.[4,7,12] Cold plasma systems are particularly interesting because they are able to operate at near room temperature, thus being suitable for processing temperature-sensitive materials.[13] Cold plasma has been used to deposit coatings that prevent bacterial adhesion and proliferation in different ways, such as releasing embedded antibacterial agents, immobilizing antibacterial molecules on the surface, and modifying the surface properties of the substrate.[12]

Although cold plasma has been usually generated by means of low-pressure technologies, atmospheric pressure plasma systems have emerged more recently as interesting alternatives because no vacuum equipment is required, their costs are lower and their implementation for in-line processing is easier.[14]

For instance, Stallard et al.[15] deposited siloxane coatings on titanium coupons through plasma polymerization using an atmospheric pressure plasma jet (APPJ) system and analyzed their effects on protein

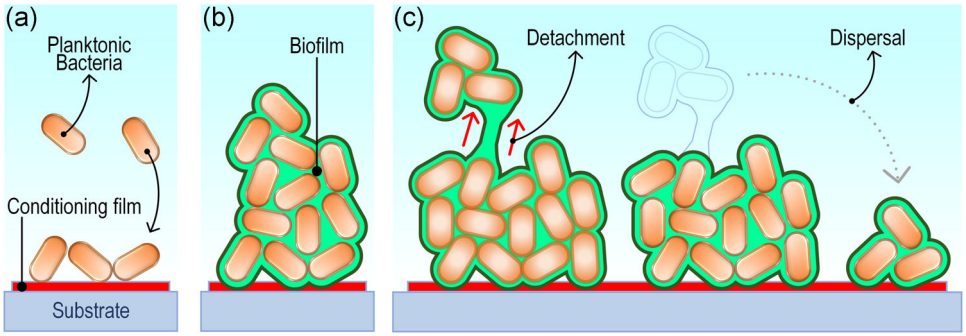

FIGURE 1 Stages of biofilm formation: (a) bacterial attachment, (b) proliferation and biofilm maturation, (c) bacterial detachment and biofilm dispersal

adsorption and bacterial attachment. They obtained coatings with different water contact angles (WCA), which ranged between <5° and 155°. The lowest levels of protein adsorption and bacterial attachment were achieved by superhydrophobic coatings (WCA > 150°) that combined a low surface energy chemistry and a nanotextured morphology. They concluded that, in those cases, the attachment of bacteria and the diffusion of proteins from the aqueous environment were reduced by the air entrapment in the surface morphology, which acted as a barrier.

In some of our most recent publications, functional coatings that were deposited by an APPJ system using acrylic acid as the precursor reduced the formation of biofilm of several bacterial species on 3D-printed[16,17] and stainless steel substrates.[18] According to our observations, the strong hydrophilic character of those coatings (WCA < 20°), which promotes the generation of a hydration layer that acts as a barrier against the attachment of bacterial cells and proteins, was the key to their effectiveness at reducing biofilm formation. As other authors have pointed, the main issue concerning plasma-polymerized acrylic acid coatings is their stability in humid environments, which has motivated several studies aimed at determining the deposition parameters that produce stable coatings with this precursor.[19–22]

As our group previously reported, resistant and stable coatings can be obtained from siloxane-based precursors, such as (3-aminopropyl)triethoxysilane (APTES).[23–25] Using APTES for the plasma polymerization in APPJ equipment produced coatings for tribological applications on thermoplastic elastomer and glass substrates, which reduced the friction coefficient and showed good wear resistance during prolonged sliding. Also, according to our findings, the physicochemical characteristics of coatings that were produced with this precursor remained practically unchanged after 1-year storage in a humid environment.[23] Furthermore, as Chen et al.[26] recently showed, plasma polymerization of APTES produces coatings with good stability in water that would be promising for applications, such as antibacterial materials, biosensors, drug immobilization in immobilization/release systems, and for improving the bioactivity and biocompatibility of implants. Nevertheless, to the best of our knowledge, no work has been published reporting the antibiofilm effects of plasma-polymerized APTES functional coatings. Therefore, the aim of this study is to reduce the biofilm formation of *P. aeruginosa* PAO1 strain through the plasma polymerization of APTES by an APPJ system using different plasma conditions. Polystyrene (PS) culture plates were used as substrates for the plasma-polymerized coatings because they are commonly used in medical research for testing bacterial adhesion and biofilm formation in vitro. Furthermore, since PS is a commonly used material in food-contact packaging, the use of these substrates is considered as a suitable initial approach to the applicability of the studied coatings in the food industry.

2 | MATERIALS AND METHODS

2.1 | Materials

PS 96-well cell culture plates (Greiner Bio-One CELLSTAR®) were used as substrates. The liquid APTES was the precursor for the deposition of coatings at the wells.

2.2 | Plasma polymerization process

An APPJ system PlasmaSpot® was used to coat the plates as depicted in Figure 2. The APPJ system consists of two cylindrical, coaxial electrodes, one of them grounded and the other one connected to a power generator that operated at a frequency of 68 kHz, with a dielectric barrier of Al_2O_3 between them. The plasma was generated with nitrogen gas (99.999%) at a flow rate of 80 slm. The plates were mounted on an X-Y table that moved under the plasma jet with a scanning movement, at a linear speed of 100 mm/s, keeping

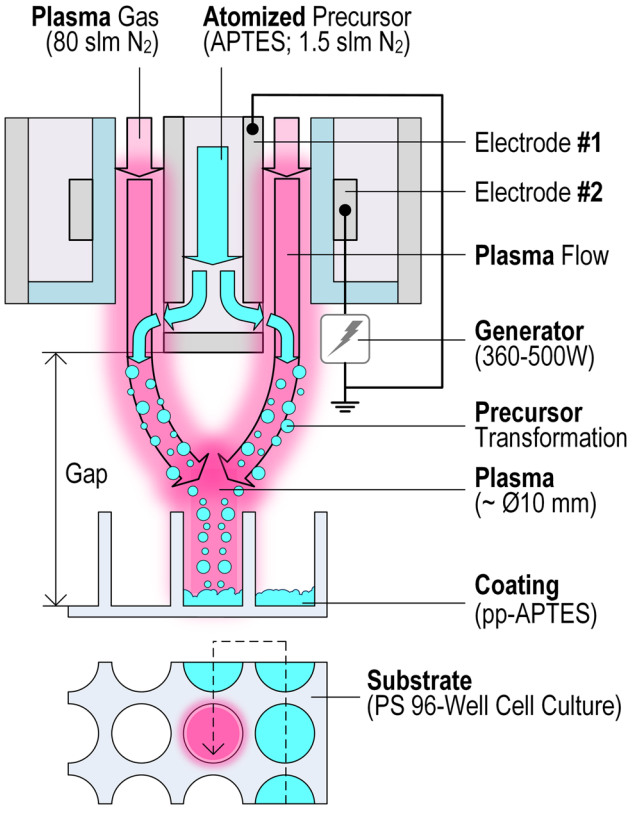

FIGURE 2 Scheme of the coating process. APTES, (3-aminopropyl)triethoxysilane

a gap of 20.9 mm between the exit of the plasma and the bottom of the wells. The track pitch of the scanning movement was equal to the spacing between consecutive columns of wells (8.9 mm) so that the plasma jet passed over the center of the wells.

The coating process consisted of two phases. In the first phase, the plates were subjected to surface activation by exposing them to one pass of the plasma jet without precursor addition. In the second phase, the plates were coated by plasma polymerization of APTES in two passes. The liquid precursor was carried by a 1.5 slm flow of nitrogen gas (99.999%), nebulized by passing through an atomizer (model 3076; TSI), and added to the afterglow. Three different settings of power at the generator (360, 440, and 500 W) were used, and each studied sample type was designated as Table 1 shows. The bottoms of several wells were extracted from the plates using a circular cutting tool to use them for the morphological and chemical characterizations of the samples, as well as for the measurement of their WCAs.

TABLE 1 Plasma power and designation of the studied samples

Sample	Power (W)
Uncoated PS	-
S360	360
S440	440
S500	500

Abbreviation: PS, polystyrene.

2.3 | Morphological characterization

The surface morphologies of the uncoated and the coated PS samples were determined by three-dimensional atomic force microscopy (AFM). Images of $40 \times 40\ \mu m$ areas of the bottom of the wells were acquired through a Multimode AFM (Bruker Corporation) with NanoScope V controller, working in tapping mode. The average roughness (R_a) of each sample was calculated as the average of three independent measurements using the software NanoScope Analysis 1.40 (Bruker Corporation). In addition, a HITACHI S-2400 scanning electron microscope (SEM) operating at 18 kV was used for the morphological characterization. The samples used for the SEM analysis were previously subjected to gold–palladium sputtering to make them conductive.

2.4 | Chemical characterization

The surface chemical compositions of the uncoated and the coated PS samples were studied by X-ray photoelectron spectroscopy (XPS) using a Kratos AXIS Supra spectrometer that was equipped with a monochromatic Al-Kα X-ray source operating at 225 W (15 mA/15 kV). The pressure in the chamber was maintained below 10^{-9} Torr. The spectrometer was set to the hybrid lens mode and the slot mode, which gave an analysis area of approximately $700 \times 300\ \mu m$. The acquisition of the XPS spectra was performed at three different locations per sample. The survey spectra for the identification of the chemical elements present in the samples were acquired at a pass energy of 160 eV. The high-resolution spectra of the regions that corresponded to specific elements were acquired at a pass energy of 20 eV. The binding energy of all the spectra was corrected by setting the highest peak of the C1s component at 285 eV. The CasaXPS 2.3.19 software was used for the correction of the binding energy and for the quantification of the atomic percentages of the elements found on the samples. The atomic percentages of the elements were calculated according to the areas under their corresponding photoelectron peaks after subtraction of a Shirley background. Deconvolution of the C1s region was carried out using the PeakFit 4.12 (SPSS Inc.) software, fitting the peaks of the deconvolution with Gaussian–Lorentzian sum functions and allowing variable widths for the peaks.

2.5 | Wettability

The wettability of the samples was studied by measuring their static WCA using the sessile drop method. Three water drops (3 μl/drop) were deposited on each sample type and their contact angles were measured by digital image analysis in the ImageJ free software[27] with the low-bond axisymmetric drop shape analysis plugin.[28] The WCA of each sample was calculated as the average value of its three respective measurements.

2.6 | Biofilm quantification

The total biofilm biomass generated by *P. aeruginosa* PAO1 strain on the different studied samples was quantified by crystal violet (CV) staining.[29] This ubiquitous bacterium is a model microorganism for the study and control of bacterial biofilms, and for that reason, it was chosen as the target pathogen to test the coatings of this study.

Eight wells of each coated and uncoated 96-well cell culture plate (Table 1) were inoculated with 200 μl of an initial 10^6 CFU/ml bacterial inoculum prepared in 3 ml of Mueller–Hinton (MH) broth (Pronadisa; Conda). To analyze the biofilm production during 1 week, the plates

were incubated at 37°C for the period from 1 to 7 days. At the end of each incubation period, the planktonic cells were removed by a quick inversion of the plate, and the biofilm was washed with phosphate-buffered saline (PBS) (200 µl/well). Subsequently, the biofilm was fixed using methanol for 15 min at room temperature. After removing the methanol, the plates were dried for 20 min at room temperature. The biofilm fixed in each well was stained with 200 µl of CV solution (10% in PBS; Sigma-Aldrich) and incubated for 10 min at room temperature. The excess CV solution was removed under running water. Finally, the CV fixed to the biofilm biomass was solubilized with 200 µl of acetic acid solution (66%, in water) and incubated at room temperature for 1 h. Absorbance was measured at 570 nm using a plate reader (POLARstar Omega microplate reader; BMG LABTECH).

3 | RESULTS AND DISCUSSION

3.1 | Morphological characterization

The surface morphology and roughness of the coatings were studied by AFM and SEM.

Figure 3 shows the average roughness values (R_a) that were obtained by AFM analysis.

The coated sample S360 showed very similar roughness values to those obtained for the uncoated PS (5.75 ± 1.13 nm), and lower than those obtained for the samples that were coated at higher powers (S440 and S500). The AFM images (Figure 4) revealed differences among the surface morphologies of the analyzed samples. On one side, the coating of sample S360 (Figure 4b) showed a smooth surface with no remarkable features. On the other hand, the samples S440 (Figure 4c) and S500 (Figure 4d) showed the formation of rougher textures, with peaks and valleys uniformly distributed all over the surface. These observations on the general morphology of the coatings were consistent with their SEM images (Figure 5). White dots were detected in SEM images, which reveal the presence of some particulates at the surface of the coated samples. The higher the plasma power, the greater the amount of particulates. As the authors reported in previous work about atmospheric pressure plasma polymerization of APTES on smooth substrates,[25] the excess gas-phase reactions that occur at high plasma powers may lead to the generation of more particulates in the coatings, and this fact would be the main cause of the roughness increase. Those particulates act as nucleation sites around which the deposited material tends to accumulate,[30,31] leading to the growth of the peaks that form the textures of samples S440 and S500. The lower plasma power used in this study for sample S360 resulted in the generation of a low amount of particulates, which caused its coating to grow more evenly and have a smoother surface. It is known that surface topography is one of the multiple factors that can influence how bacteria interact with surfaces. As discussed in our previous work where antibiofilm coatings with R_a in the ranges of 373–503 nm[16] and 398–560 nm[17] were produced, the generation of different topographies has different effects. For instance, rough surfaces can magnify surface hydrophilicity to the point that bacterial cells are repelled by surface hydration, and they can reduce the contact area between the bacteria and the surfaces. Nevertheless, it is worth considering the fact that the surface features of samples S440 and S500, as well as the R_a values of all the studied samples of the present work, were much smaller than the reported size of *P. aeruginosa* bacteria (rods of 0.5–0.8 µm in width and 1.5–3 µm in length).[32] Furthermore, the samples that were studied in this work were much smoother than those of our previous work, as their smaller R_a values show, which are in a much narrower range (5.75–10.47 nm). Therefore, an influence of the observed morphological differences on the interaction of these surfaces with bacterial cells, and on biofilm formation, seems unlikely.

3.2 | Chemical characterization

XPS analysis was carried out to identify the differences between the surface chemistries of the uncoated and the coated PS plates, as well as to determine if the plasma power influenced those chemistries.

As shown in Table 2, the main elements that were detected on the uncoated PS surface were carbon and oxygen, as well as a small amount of nitrogen that may be due to the treatment applied to the cell culture plates by the manufacturer. These results are consistent with previously

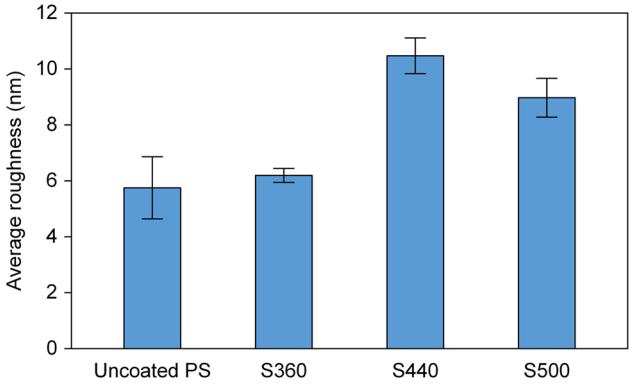

FIGURE 3 Average roughness (R_a) of the uncoated and coated samples. PS, polystyrene

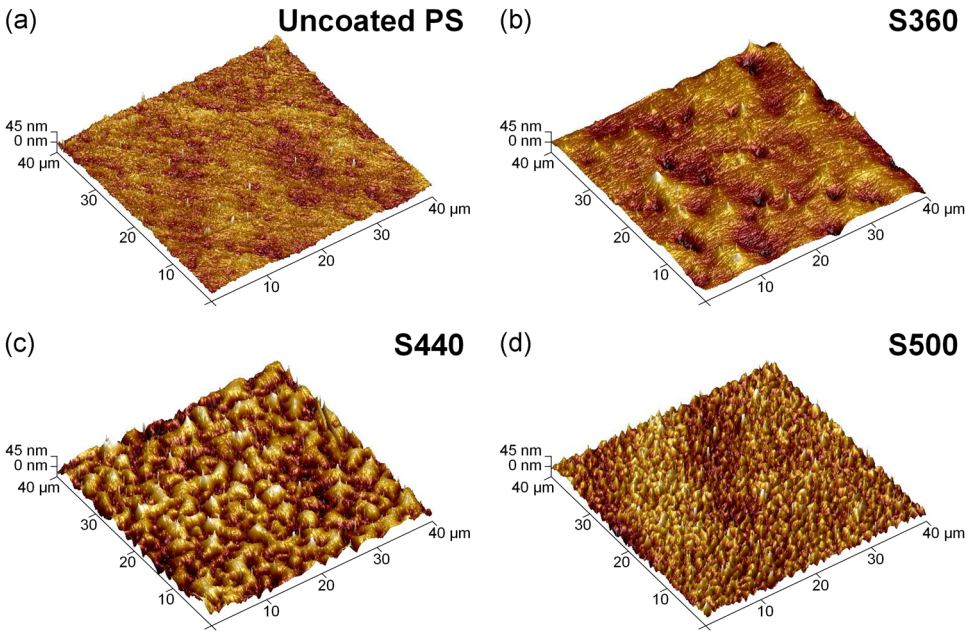

FIGURE 4 Atomic force microscopy images of the uncoated and coated samples. PS, polystyrene

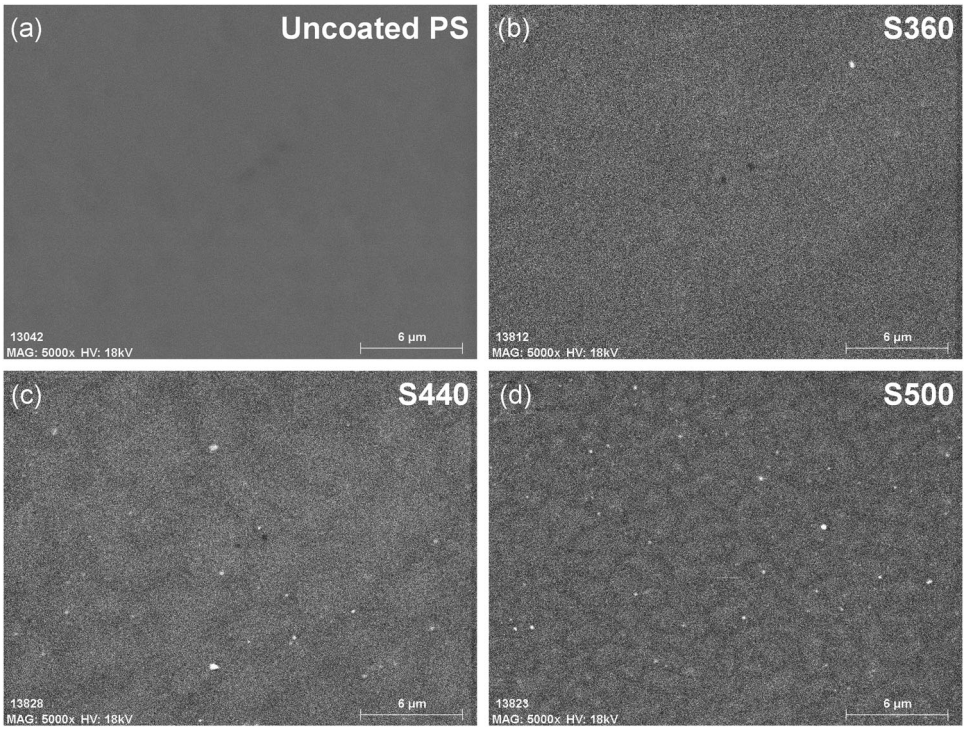

FIGURE 5 Scanning electron microscopy images of the uncoated and coated samples at a magnification of ×5000. PS, polystyrene

reported chemical characterization of PS culture plates subjected to nitrogen plasma treatment.[33]

The elements detected at the surface of the coatings were those provided by the APTES molecule (Figure 6), that is, carbon, oxygen, silicon, and nitrogen. The surfaces of the coated samples showed lower carbon percentages and higher oxygen, silicon, and nitrogen percentages than the uncoated PS ones. In the coated samples, the carbon abundance decreased and the oxygen abundance increased when the plasma power increased. This behavior can be caused by an increase in the chain-scission of the precursor and the formation of gases, such as CO and CO_2.[25,34]

Oxygenated carbon groups induce oxidative stress,[35] which affects the bacterial response and may lead to

TABLE 2 Atomic percentage of C, O, Si, and N on the surfaces of the analyzed samples

Sample	Elemental composition (at%)			
	C1s	O1s	Si2p	N1s
Uncoated PS	86 ± 0.4	12.9 ± 0.3	-	1.1 ± 0.1
S360	59.1 ± 5.7	27.5 ± 4.4	9.2 ± 1.5	4.2 ± 1.1
S440	55 ± 3.6	29.8 ± 2.3	9.1 ± 1.9	6.1 ± 0.6
S500	47.8 ± 0.3	35.1 ± 0.4	12.3 ± 0.2	4.8 ± 0.2

Abbreviation: PS, polystyrene.

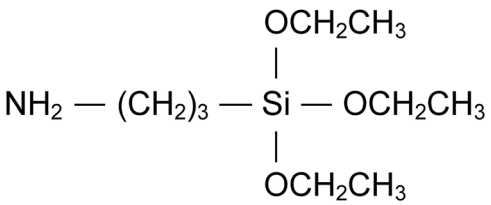

FIGURE 6 Chemical structure of (3-aminopropyl) triethoxysilane (APTES)

antibacterial effects. Deconvolution of the C1s signal was carried out to identify and quantify its oxygen-containing functional groups. Table 3 shows the chemical groups that were considered in the deconvolution and their respective binding energies. The C1s signal of the uncoated PS sample (Figure 7a) contained the following components: (i) C–C and C–H bonds of aromatic carbon, (ii) C–C and C–H bonds of aliphatic carbon, (iii) C–O and C–N bonds, (iv) C═O bonds from ketones and amides, (v) COO groups, and the (vi) π–π* shake-up that is associated with the aromatic rings of PS.[33] The C1s signal of the coated samples (Figure 7b,c) contained the components (ii), (iii), (iv), and (v), as well as (vii) C–Si bonds that were provided by the plasma polymerization of APTES.

The presence of oxygen-containing functional groups on each sample was quantified as the addition of the detected abundance linked to peaks (iii), (iv), and (v). As Figure 8 shows, the coated samples showed an increase in the abundance of oxygen-containing groups in comparison with the uncoated PS samples. Furthermore, in the coated samples, the percentage of oxygen-containing groups slightly decreased when the plasma power increased. This is probably related to the aforementioned chain-scission that caused a decrease in the carbon content of the coatings.

3.3 | WCA measurements

The wettability of a surface is one of the factors that influence bacterial adhesion. Hydrophobic (WCA > 90°) and superhydrophobic (WCA > 150°) characters are favorable to achieve antibacterial effects because the adhesion of bacteria to the surface and the biofilm production weakens.[12] Also, as discussed in our previous publications, strong hydrophilic surfaces (WCA < 20°) can reduce biofilm formation through the generation of a hydration layer that acts as a barrier against the attachment of bacterial cells and proteins.[16–18]

TABLE 3 Components of the deconvolution of the C1s signal and their binding energies

	Groups	Binding energy (eV)	References
(i)	C–C, C–H (aromatic)	~284.6	[33]
(ii)	C–C, C–H (aliphatic)	~285	[23,33]
(iii)	C–O, C–N	~286.6	[23,33]
(iv)	C═O	~288	[23,33]
(v)	COO	~289.3	[33]
(vi)	π–π* shake-up	~291.2	[33]
(vii)	C–Si	~284.3	[23]

The static WCA was measured to determine the wetting characters of the samples. As Figure 9 shows, the uncoated PS samples had a WCA of 36.2 ± 8.3°, which is unexpectedly low considering that PS surfaces are usually hydrophobic. This low WCA value is explained by the fact that the cell culture plates had been plasma-treated by their manufacturer. Furthermore, this is consistent with previously published work in which untreated PS culture plates had a WCA of ~71° and, after being subjected to plasma treatments, their WCA was ≤44°.[33] On the contrary, all coated PS samples of the present work showed similar WCA values (ranging from 53.6 ± 7.6° to 58.5 ± 4.73°) that were higher than that of the uncoated PS. Although all the studied samples exhibited a hydrophilic character (i.e., WCA < 90°), this was not as strong as in our previous work (WCA < 20°). For that reason, in the present work, there were no significant differences in the wettability of the samples to explain possible variations in their interaction with bacteria and in the generation of biofilm.

3.4 | Biofilm measurements

The total biofilm biomass generated by *P. aeruginosa* on the uncoated and coated PS surfaces was quantified daily for a week. Figure 10 shows the relative biofilm production of *P. aeruginosa* PAO1 strain for each coated sample in comparison to the uncoated PS samples (considered as the reference with 100% biofilm

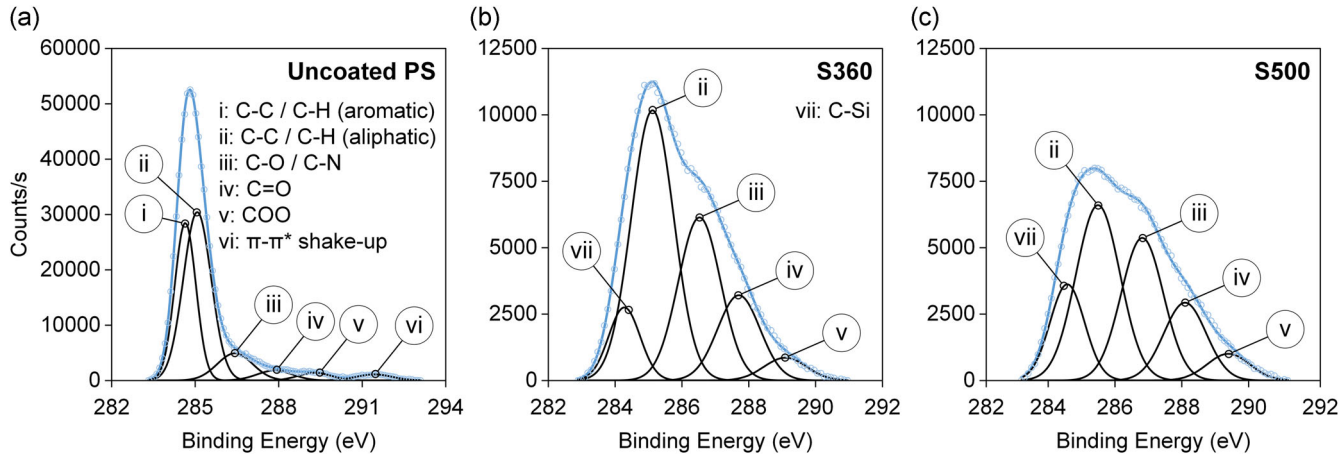

FIGURE 7 Deconvolution of the C1s signal of the following samples: (a) uncoated PS, (b) S360, and (c) S500. PS, polystyrene

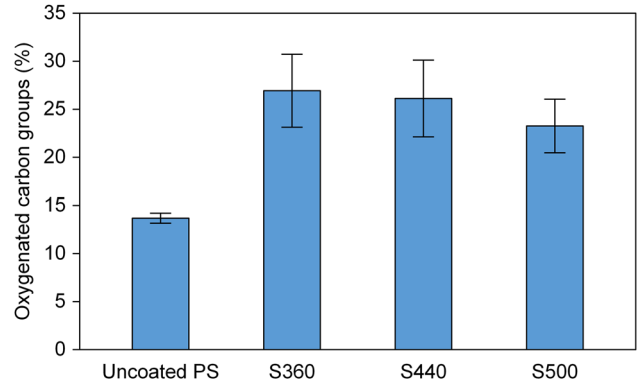

FIGURE 8 Total percentages of oxygen-containing groups on the uncoated and the coated polystyrene (PS) samples, obtained by deconvolution of the C1s signal

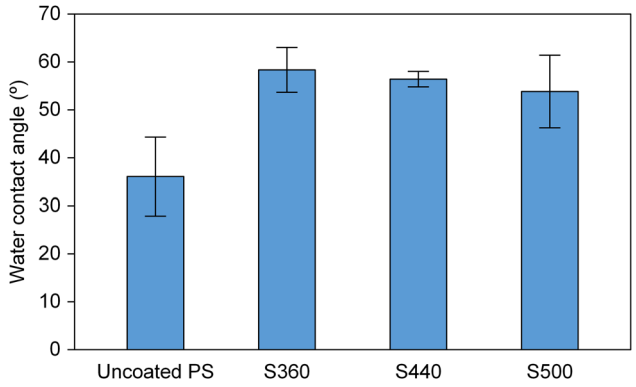

FIGURE 9 Water contact angle of the uncoated and coated samples. PS, polystyrene

production). High biofilm biomass (>200%) was produced on the coated samples during the first days of incubation, reaching their maximum values after 2 days of incubation. Then, the biofilm production decreased to values under the reference samples. At the end of the week, all the coated samples showed a relative biofilm production <100%.

As the chemical characterization revealed, the coated samples showed a higher abundance of oxygenated carbon functional groups than the uncoated PS samples (Figure 8), which have been reported as oxidative stress inductors.[35] In this way, some authors identified that *P. aeruginosa* can overproduce EPS when it is exposed to oxygen radicals, as a protection mechanism against oxidative stress.[36,37] Therefore, the increased biofilm production observed during the first 2 days could be caused by higher production of EPS in response to higher levels of oxidative stress produced by bacterial contact with the coatings.

Additionally, as previously reported,[38] amine groups ($-NH_2$) are basic groups that, in the presence of adsorbed water molecules, accept a proton and generate positively charged sites. *P. aeruginosa* bacteria are negatively charged, thus, an electrostatic attraction occurs between bacteria and the positively charged sites of the coatings, favoring bacterial attachment. Therefore, another possible reason for the higher initial biofilm production on the coated samples of the present work can be the amine groups of the APTES molecule (Figure 6). This is consistent with the higher atomic percentages of nitrogen (Table 2) detected on the coated samples (ranging from $4.2 \pm 1.1\%$ to $6.1 \pm 0.6\%$) than on the uncoated PS samples ($1.1 \pm 0.1\%$). Electrostatic attraction between amine groups and the first planktonic bacteria attached could have increased the adhesion (Figure 11a) and the subsequent biofilm formation during the first days of incubation. On the contrary, it has been argued in the bibliography that amine groups are usually released from amine-containing coatings as a result of aging in ambient air and dissolution in water; and that these amines can have toxic effects, thus being deleterious for cell

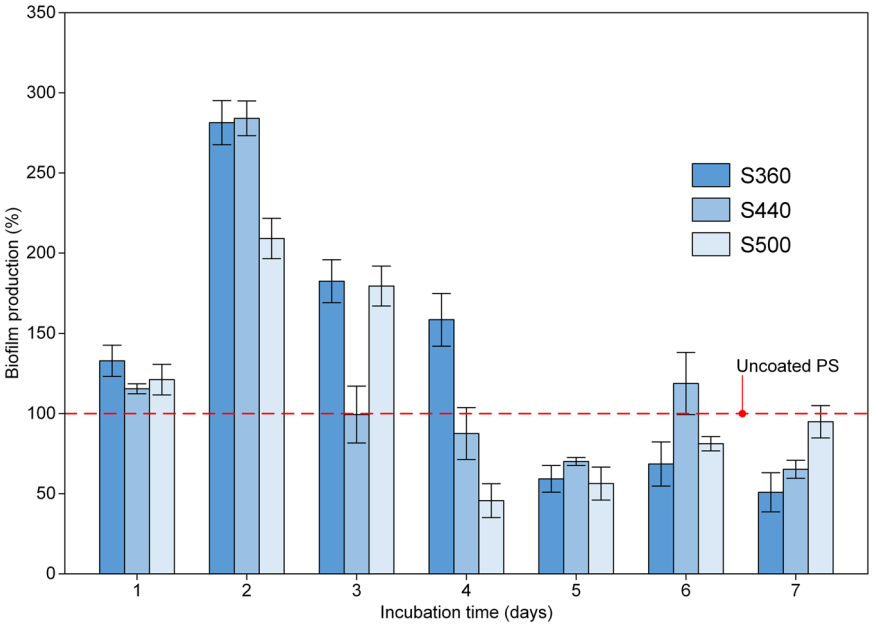

FIGURE 10 Relative biofilm production for the coated polystyrene (PS) samples during 7 days in comparison to uncoated PS samples

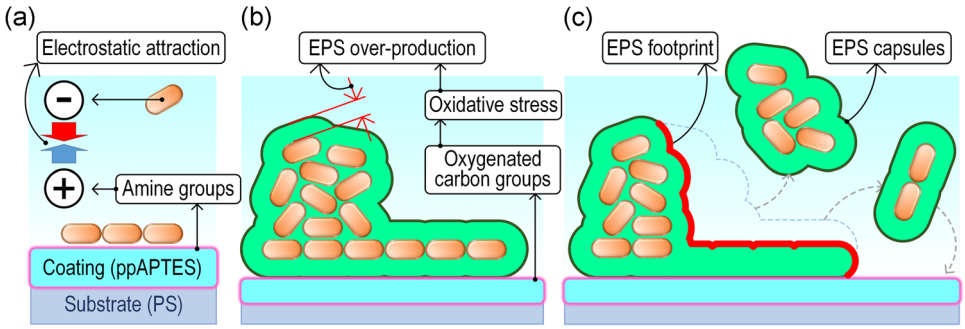

FIGURE 11 Evolution of the interaction between the coatings and bacteria during incubation: (a) initial promotion of bacterial attachment to the coatings through electrostatic attraction, (b) EPS overproduction during early biofilm formation due to the oxidative stress induced by oxygenated carbon groups, and (c) inhibition of further bacterial attachment and biofilm formation by EPS footprints and capsules. APTES, (3-aminopropyl)triethoxysilane; EPS, extracellular polymeric substances; PS, polystyrene

growth.[39] The possibility that the aforementioned occurs with the coatings of the present work cannot be denied at the current state of our research. Nevertheless, considering the importance of nontoxicity for biomedical and food-related applications, an in-depth safety study is planned for future work to identify and evaluate any possible toxic effects of the coatings.

The decrease in bacterial biofilm production on the coated samples after the first 2 days (Figure 10) suggests that the mechanism of biofilm formation on these samples was different from that on uncoated PS samples. One of the causes could be the EPS production because it has been reported that EPS produced by *P. aeruginosa* can avoid bacterial adhesion.[40] In the detachment phase, *P. aeruginosa* leaves an EPS footprint that covers the surface and discourages bacterial adhesion after several cycles of detachment and redeposition.[41] Furthermore, EPS expression can cover bacteria into a capsule of polysaccharides, protecting the adhesins and other bacterial surface features required to interact with other surfaces,[42–44] and subsequently inhibiting bacterial attachment, aggregation, and biofilm formation.

Considering all these data, our results could suggest that the higher biofilm abundance produced on the coated samples during the first 2 days was linked to higher concentrations of oxygenated carbon groups, higher oxidative stress, and subsequently higher EPS production (Figure 11b). This could in fact cause the formation of greater footprints at the surface of the coatings and capsules around the detached bacteria during the stage of biofilm dispersal. Then, these footprints and capsules avoided bacterial attachment and biofilm formation at subsequent cycles (Figure 11c). As a consequence, the relative biofilm production decreased on

all coated samples after longer periods of incubation, being <100% after 7 days.

This reasoning is supported when the biofilm productions after 2 and 7 days of incubation are compared. It seems that the considerably higher biofilm abundances on samples S360 and S440 after 2 days (281.4 ± 13.8% and 284.1 ± 10.9%, respectively) in comparison with that of sample S500 (209.1 ± 12.6%), led to lower biofilm abundances after 7 days. Thus, whereas the biofilm abundance after 7 days on sample S500 was 94.9 ± 10.1%, those on samples S360 and S440 were reduced to 50.9 ± 12.2% and 65.2 ± 5.6%, respectively.

4 | CONCLUSIONS

PS substrates were coated by atmospheric pressure plasma polymerization of APTES. Different coatings were deposited using different plasma powers. The morphology, roughness, surface chemistry, and wettability of the coatings were analyzed, and their effect on biofilm formation by *P. aeruginosa* PAO1 strain was studied during 7 days of incubation.

A reduction of the *P. aeruginosa* biofilm formation was observed on coated samples in long term. It could be suggested that the initial EPS overproduction on the surface of the coatings caused the inhibition of biofilm formation in long term. The main cause of this behavior seems to be the higher concentrations of oxygenated carbon groups on the coatings, which induced higher levels of oxidative stress on the bacteria in contact with them. As a response to this higher oxidative stress, those bacteria produced higher amounts of EPS during the first days of incubation. Afterward, this could cause the formation of greater EPS footprints on the surface of the coatings, and EPS capsules around the detached bacteria, at the biofilm dispersal phase. Thus, these footprints and capsules avoided further bacterial attachment and biofilm formation at subsequent cycles.

Sample S360, which was coated with the lowest plasma power (360 W) that was used in this study, showed the lowest relative biofilm production (50.9 ± 12.2%) after 7 days of incubation.

APTES was used as the precursor for the coatings of this study because, as the authors observed in previous work, siloxanes are suitable for the deposition of resistant and stable coatings.[23–25] Future research will aim to verify the suitability of these coatings over other antibacterial approaches in terms of their adhesion, resistance to abrasion, and stability in humid environments. Furthermore, to ascertain the safety of these coatings, an evaluation of their possible toxicity through lactate dehydrogenase leakage assays is planned for the upcoming stages of this research project.

ACKNOWLEDGMENTS

XPS tests were conducted by the Advanced Microscopy Laboratory (LMA) of The Institute of Nanoscience of Aragón (INA), University of Zaragoza. The authors are thankful to the LMA-INA for the access to their equipment and their expertise. The AFM images were taken by the Central Research Support Service (SCAI) of the University of Málaga (UMA). The author Elisa Sainz-García, a postdoctoral researcher of the University of La Rioja, thank the postdoctoral training program that is funded by the Plan Propio of the University of La Rioja. The authors Ignacio Muro-Fraguas and Ana Sainz-García are thankful to the program of pre-doctoral contracts for the training of research staff that is funded by the University of La Rioja. This study was funded by the Programa Estatal de Investigación, Desarrollo e Innovación Orientada a los Retos de la Sociedad through the project PID2020-113658RB-C21.

CONFLICT OF INTERESTS

The authors declare that there are no conflict of interests.

DATA AVAILABILITY STATEMENT

Research data are not shared.

ORCID

Rodolfo Múgica-Vidal http://orcid.org/0000-0003-2150-4032
Elisa Sainz-García http://orcid.org/0000-0001-5776-0455
Ignacio Muro-Fraguas http://orcid.org/0000-0001-8255-926X
Ana Sainz-García http://orcid.org/0000-0003-3973-6704
Ana González-Marcos http://orcid.org/0000-0003-4684-659X
María López http://orcid.org/0000-0002-3834-4891
Beatriz Rojo-Bezares http://orcid.org/0000-0003-2742-0980
Paula Toledano http://orcid.org/0000-0001-8586-8607
Yolanda Sáenz http://orcid.org/0000-0002-2457-4258
Fernando Alba-Elías http://orcid.org/0000-0002-3918-0155

REFERENCES

[1] B. Dong, H. Jiang, S. Manolache, A. C. L. Wong, F. S. Denes, *Langmuir* **2007**, *23*, 7306.
[2] A. A. Gabriel, M. C. C. F. Ugay, M. A. T. Siringan, L. M. D. Rosario, R. B. Tumlos, H. J. Ramos, *Innovative Food Sci. Emerging Technol.* **2016**, *36*, 311.
[3] S. A. Ermolaeva, E. V. Sysolyatina, A. L. Gintsburg, *Biointerphases* **2015**, *10*, 029404.
[4] S. Bhatt, J. Pulpytel, F. Arefi-Khonsari, *Surf. Innovations* **2015**, *3*, 63.

[5] M. Chen, Q. Yu, H. Sun, *Int. J. Mol. Sci.* **2013**, *14*, 18488.
[6] Z. Kovalova, M. Leroy, M. J. Kirkpatrick, E. Odic, Z. Machala, *Bioelectrochemistry* **2016**, *112*, 91.
[7] M. Moreno-Couranjou, R. Mauchauffé, S. Bonot, C. Detrembleur, P. Choquet, *J. Mater. Chem. B* **2018**, *6*, 614.
[8] M. Y. Alkawareek, Q. T. Algwari, G. Laverty, S. P. Gorman, W. G. Graham, D. O'Connell, B. F. Gilmore, *PLOS One* **2012**, *7*, e44289.
[9] L. Guo, W. Yuan, Z. Lu, C. M. Li, *Colloids Surf., A* **2013**, *439*, 69.
[10] K. Vasilev, S. S. Griesser, H. J. Griesser, *Plasma Processes Polym.* **2011**, *8*, 1010.
[11] T. T. Gupta, S. B. Karki, J. S. Matson, D. J. Gehling, H. Ayan, *BioMed Res. Int.* **2017**, *2017*, e6085741.
[12] E. Sardella, F. Palumbo, G. Camporeale, P. Favia, *Materials (Basel)* **2016**, *9*, 515.
[13] D. Merche, N. Vandencasteele, F. Reniers, *Thin Solid Films* **2012**, *520*, 4219.
[14] M. C. Ramkumar, K. Navaneetha Pandiyaraj, A. Arun Kumar, P. V. A. Padmanabhan, P. Cools, N. De Geyter, R. Morent, S. Uday Kumar, V. Kumar, P. Gopinath, S. K. Jaganathan, R. R. Deshmukh, *Surf. Coat. Technol.* **2017**, *329*, 55.
[15] C. P. Stallard, K. A. McDonnell, O. D. Onayemi, J. P. O'Gara, D. P. Dowling, *Biointerphases* **2012**, *7*, 31.
[16] I. Muro-Fraguas, A. Sainz-García, P. Fernández Gómez, M. López, R. Múgica-Vidal, E. Sainz-García, P. Toledano, Y. Sáenz, M. López, M. González-Raurich, M. Prieto, A. Alvarez-Ordóñez, A. González-Marcos, F. Alba-Elías, *Innovative Food Sci. Emerging Technol.* **2020**, *64*, 102404.
[17] I. Muro-Fraguas, A. Sainz-García, M. López, B. Rojo-Bezares, R. Múgica-Vidal, E. Sainz-García, P. Toledano, Y. Sáenz, A. González-Marcos, F. Alba-Elías, *Surf. Coat. Technol.* **2020**, *399*, 126163.
[18] P. Fernández-Gómez, I. Muro-Fraguas, R. Múgica-Vidal, A. Sainz-García, E. Sainz-García, M. González-Raurich, A. Álvarez-Ordóñez, M. Prieto, M. López, M. López, P. Toledano, Y. Sáenz, A. González-Marcos, F. Alba-Elías, *Food Res. Int.* **2020**, *136*, 109508.
[19] R. Jafari, M. Tatoulian, F. Arefi-Khonsari, *React. Funct. Polym.* **2011**, *71*, 520.
[20] O. Carton, D. Ben Salem, J. Pulpytel, F. Arefi-Khonsari, *Plasma Chem. Plasma Process.* **2015**, *35*, 819.
[21] P. Bosso, F. Fanelli, F. Fracassi, *Plasma Processes Polym.* **2016**, *13*, 217.
[22] P. Cools, H. Declercq, N. De Geyter, R. Morent, *Appl. Surf. Sci.* **2018**, *432*, 214.
[23] E. Sainz-García, F. Alba-Elías, R. Múgica-Vidal, A. González-Marcos, *Appl. Surf. Sci.* **2015**, *328*, 554.
[24] E. Sainz-García, F. Alba-Elías, R. Múgica-Vidal, M. Pantoja-Ruiz, *Appl. Surf. Sci.* **2016**, *371*, 50.
[25] R. Múgica-Vidal, F. Alba-Elías, E. Sainz-García, A. González-Marcos, *Surf. Coat. Technol.* **2017**, *309*, 1062.
[26] Z. Chen, J. Zhao, C. Jin, Y. Yuan, Y. Zhang, M. Tatoulian, X. Rao, *Mater. Lett.* **2020**, *264*, 127350.
[27] C. A. Schneider, W. S. Rasband, K. W. Eliceiri, *Nat. Methods* **2012**, *9*, 671.
[28] A. F. Stalder, T. Melchior, M. Müller, D. Sage, T. Blu, M. Unser, *Colloids Surf., A* **2010**, *364*, 72.
[29] E. Peeters, H. J. Nelis, T. Coenye, *J. Microbiol. Methods* **2008**, *72*, 157.
[30] B. Borer, R. von Rohr, *Surf. Coat. Technol.* **2005**, *200*, 377.
[31] B. Borer, *SiO_x in a Thin Film Deposition on Particles by Plasma Enhanced Chemical Vapor Deposition Circulating Fluidized Bed Reactor*, Swiss Federal Institute of Technology, Zurich **2005**.
[32] A. Tripathy, P. Sen, B. Su, W. H. Briscoe, *Adv. Colloid Interface Sci.* **2017**, *248*, 85.
[33] O. M. Ba, P. Marmey, K. Anselme, A. C. Duncan, A. Ponche, *Colloids Surf., B* **2016**, *145*, 1.
[34] K. Sever, Y. Seki, H. A. Güleç, M. Sarikanat, M. Mutlu, I. Tavman, *Appl. Surf. Sci.* **2009**, *255*, 8450.
[35] S. Das, S. Singh, V. Singh, D. Joung, J. M. Dowding, D. Reid, J. Anderson, L. Zhai, S. I. Khondaker, W. T. Self, S. Seal, *Part. Part. Syst. Charact.* **2013**, *30*, 148.
[36] K. Mathee, O. Ciofu, C. Sternberg, P. W. Lindum, J. I. A. Campbell, P. Jensen, A. H. Johnsen, M. Givskov, D. E. Ohman, S. Molin, N. Høiby, A. Kharazmi, *Microbiology* **1999**, *145*, 1349.
[37] M. Hentzer, G. M. Teitzel, G. J. Balzer, A. Heydorn, S. Molin, M. Givskov, M. R. Parsek, *J. Bacteriol.* **2001**, *183*, 5395.
[38] M. E. Villanueva, A. Salinas, G. J. Copello, L. E. Díaz, *Surf. Coat. Technol.* **2014**, *254*, 145.
[39] D. Hegemann, *Thin Solid Films* **2015**, *581*, 2.
[40] G. Hwang, S. Kang, M. G. El-Din, Y. Liu, *Biofouling* **2012**, *28*, 525.
[41] C. Gómez-Suárez, J. Pasma, A. J. van der Borden, J. Wingender, H. C. Flemming, H. J. Busscher, H. C. van der Mei, *Microbiology* **2002**, *148*, 1161.
[42] M. A. Schembri, D. Dalsgaard, P. Klemm, *J. Bacteriol.* **2004**, *186*, 1249.
[43] M. Herzberg, T. Z. Rezene, C. Ziemba, O. Gillor, K. Mathee, *Environ. Sci. Technol.* **2009**, *43*, 7376.
[44] O. Orgad, Y. Oren, S. L. Walker, M. Herzberg, *Biofouling* **2011**, *27*, 787.

How to cite this article: R. Múgica-Vidal, E. Sainz-García, I. Muro-Fraguas, A. Sainz-García, A. González-Marcos, M. López, B. Rojo-Bezares, P. Toledano, Y. Sáenz, F. Alba-Elías. Inhibition of biofilm formation on polystyrene substrates by atmospheric pressure plasma polymerization of siloxane-based coatings. *Plasma Processes Polym.* **2021**;18:e2100097.
https://doi.org/10.1002/ppap.202100097